

High-Pressure Structural Evolution of Disordered Polymeric CS₂

Jinwei Yan, Ondrej Tóth, Wan Xu, Xiao-Di Liu, Eugene Gregoryanz, Philip Dalladay-Simpson, Zeming Qi, Shiyu Xie, Federico Gorelli, Roman Martoňák, and Mario Santoro*

Cite This: *J. Phys. Chem. Lett.* 2021, 12, 7229–7235

Read Online

ACCESS |



Metrics & More

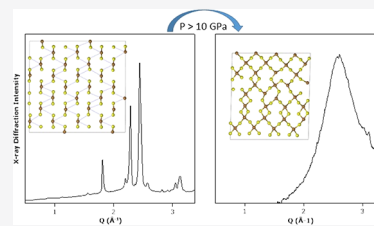


Article Recommendations



Supporting Information

ABSTRACT: Carbon disulfide is an archetypal double-bonded molecule belonging to the class of group IV–group VI, AB₂ compounds. It is widely believed that, upon compression to several GPa at room temperature and above, a polymeric chain of type $-(C=S)-S-$,_n named Bridgman's black polymer, will form. By combining optical spectroscopy and synchrotron X-ray diffraction data with ab initio simulations, we demonstrate that the structure of this polymer is different. Solid molecular CS₂ polymerizes at ~10–11 GPa. The polymer is disordered and consists of a mixture of 3-fold (C3) and 4-fold (C4) coordinated carbon atoms with some C=C double bonds. The C4/C3 ratio continuously increases upon further compression to 40 GPa. Upon decompression, structural changes are partially reverted, while the sample also undergoes partial disproportionation. Our work uncovers the nontrivial high-pressure structural evolution in one of the simplest molecular systems exhibiting molecular as well as polymeric phases.



Carbon disulfide belongs to the important class of IV–VI, AB₂ compounds. The general high-pressure trend of these compounds is to increase the coordination of the cation by the anion in typical pressure ranges of several to tens of GPa. Indeed, it is well established that the coordination goes from 4 to 6 in SiO₂,^{1–3} GeO₂,^{4,5} and SiS₂,^{6–8} and from 2 to mixed 3–4 and pure 4 in nonmolecular amorphous and crystalline CO₂, respectively.^{9–15} Furthermore, in the multi-Mbar, CO₂ is also predicted to exhibit 6-fold coordination.¹⁶ At variance with the above-mentioned systems, CS₂ is a strongly metastable substance, even in the molecular state under ambient conditions. Several works reported the high-pressure formation of extended solids obtained by compressing molecular CS₂ above several GPa,^{17–22} yet determining the chemical nature and structure of these materials, which is critical in fully understanding the family of group IV–VI AB₂ compounds, has remained elusive. In the pioneering study by Bridgman¹⁷ at temperature of 448 K, an irreversible transition to a black form was observed at 4.5 GPa and it was suggested that the material has a structure similar to that of SiO₂. A subsequent IR spectroscopy study by Whalley¹⁸ under similar conditions (5.5 GPa at 458 K) suggested that the black color and the IR spectrum are compatible with the material being a linear polymer, $-(C=S)-S-$,_n named Bridgman's black polymer (BBP), where carbon is in a planar 3-fold coordination by sulphur. Butcher et al.,¹⁹ mapped the P–T formation diagram and also performed XRD and electron diffraction experiments, concluding that the high-pressure CS₂ has a disordered structure. Chan and Jonscher²⁰ observed the transformation at 3.3 GPa and temperature of 523 K and employed infrared (IR) spectroscopy, optical spectroscopy, X-ray diffraction (XRD), and other methods. They proposed the existence of two forms. form A was suggested to be a ladder

polymer with 3-coordinated carbon atoms, obtained by cross-linking two BBP linear chains via creating S–S bonds, while form B was proposed to consist of a subsulfide (possibly C₂S₃) and free sulfur. Agnew et al. studied the transformation at room temperature where it occurs at >8.3 GPa, also by IR spectroscopy, and the product was interpreted as a mixture of the BBP and CS₂ dimers.²¹ It is important to note, however, that all above interpretations of the polymer were not grounded on quantitative structural models and were derived from a limited dataset. More recently, CS₂ was investigated up to 90 GPa by Raman spectroscopy, X-ray diffraction (XRD), and ab initio calculations,²² proposing the polymerization to a disordered form with 3-fold coordinated C atoms of ~9 GPa and an additional structural transformation to a form with 4-fold coordinated C atoms around 30 GPa. On the other hand, the reported Raman spectra hardly demonstrated any major changes above 9 GPa. Metallization and superconductivity have also been reported above 50 GPa.^{22,23}

Concerning theoretical studies, various CS₂ oligomers were studied in ref 24, where it was concluded that a hypothetical condensed CS₂ phase may present four-connected carbon atoms (oligomer 12b). Subsequently, a constrained (no C–C or S–S bonds) first-principles evolutionary search was conducted up to 200 GPa in order to identify the lowest-enthalpy structures of nonmolecular CS₂ with C in 4-fold coordination by S,²⁵ yet the structure of the experimentally

Received: June 3, 2021

Accepted: July 23, 2021

Published: July 26, 2021



obtained extended, disordered CS₂ remained unsolved. In another ab initio simulation study with fixed C:S = 1:2 stoichiometry, the molecular crystal has been predicted to transform to various nonmolecular either amorphous or crystalline solids, at >10 GPa.²⁶ In a recent study,²⁷ the structural search was performed at 2, 60, and 100 GPa, focusing on possible superconducting phases. All phases found in the unconstrained studies^{26,27} include C–C and S–S bonds along with C–S bonds, and also C and S are predicted to separate on the spatial scale of the simulation cell. Lacking detailed comparison with experimental data, however, none of the existing studies allows one to determine the structure of polymeric CS₂ in a conclusive manner, leaving it as an open problem.

Here, we present a combined experimental and computational study based on Raman and synchrotron IR spectroscopy, synchrotron X-ray diffraction (XRD), ab initio molecular dynamics simulations, and crystal structure prediction, aimed at uncovering the structure of polymeric CS₂ at 0–40 GPa. We find that this material is far more complex than the simple Bridgman's polymer, because it consists of a strongly pressure-dependent mixture of C sites in 3-fold and 4-fold coordination by S as well as chains with C=C double bonds. Our experimental and computational methods are described in the Supporting Information (see also refs 28–35).

Optical, vibrational spectroscopies are a key tool for a clear identification of pressure-driven changes in the chemical nature of the sample. In Figure 1A, we report selected Raman spectra of solid CS₂ measured upon increasing and decreasing pressure in the 0–40 GPa pressure range. In the 0–8 GPa range, we only observe sharp and intense peaks related to the molecular and lattice modes of the CS₂ crystal. Above 9–10 GPa, the sample becomes opaque, and the spectrum modifies significantly and abruptly: the sharp peaks are entirely replaced by at least six much broader and weaker bands marked as “a”, “b”, “c”, “d”, “e”, and “f” at ~130, 490, 740–750, 870, 1060, and 1480 cm⁻¹, respectively, signaling a major chemical modification, such as the formation of a polymeric and likely disordered form. We note that previous Raman investigations reported only band “b”.²² These new bands undergo partially reversible intensity changes along the pressure cycle. Indeed, band “a” decreases substantially upon increasing pressure to 40 GPa, and it increases back when the pressure is reduced. Similarly, bands “e” and “f” reversibly decrease upon increasing pressure, and band “f” becomes the dominant peak upon returning to ambient pressure. Bands “b”, “c”, and “d” are always observed along the pressure cycle, except upon decreasing pressure below 14 GPa, where bands “c” and “d” become hardly detectable. In Figure 1B, we report selected medium IR absorption spectra of CS₂ measured at 600–1800 cm⁻¹, along a typical pressure cycle in the 4–37 GPa range. Comparison to Raman spectra clearly shows that the two types of spectra for polymeric CS₂, IR and Raman, have very similar bands in the common frequency range, while the IR bands are observed with a much higher signal-to-noise ratio. We then adopt the same Raman labels for the main IR peaks of polymeric CS₂: bands “c”, “d”, “e”, and “f”. Similarly to Raman spectroscopy, the IR spectrum has an entirely molecular origin at 5 GPa, as testified by the strong saturating peak at ~1500 cm⁻¹, which is assigned to the antisymmetric CS₂ stretching mode. The spectrum undergoes sudden and major changes upon increasing pressure above 9–10 GPa, pointing to the formation of a polymeric product. In fact, the molecular peak is

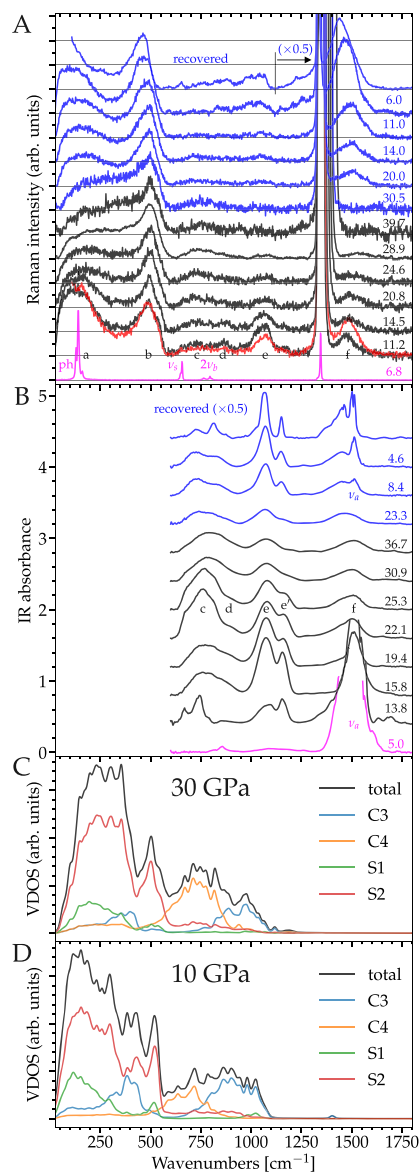


Figure 1. (A and B) Selected experimental Raman (panel (A)) and IR (panel (B)) spectra of CS₂, measured upon increasing (magenta and black) and subsequently decreasing (blue) pressure. Laser wavelength for Raman spectroscopy: 660 nm. Sharp ν_s and $2\nu_b$ peaks in Raman and strong saturating ν_a peak in IR: lattice, symmetric molecular stretching, double (overtone) molecular bending, and asymmetric molecular stretching modes of the CS₂ molecular crystal, respectively. Broad “a”–“f” peaks: peaks of polymeric CS₂. Red line: Raman spectrum measured on a similar sample using the 532 nm laser line. For the sake of clarity, Raman spectra of polymeric CS₂ have been vertically rescaled by the same intensity of peak “b”, while the Raman spectrum of molecular CS₂ is rescaled by a factor of ~10. Raman and IR spectra have also been vertically shifted. (C and D) total and partial vibrational density of states (VDOS) calculated for two different pressures from configurations obtained in ab initio MD. Lines of different colors indicate different C and S sites (see text).

replaced by nonmolecular broad bands “c”, “d”, “e”, “e'”, and “f”. Under closer inspection, band “c” exhibits a complex structure consisting of multiple contributions at some pressures, while bands “e” and “e'” reversibly decrease upon increasing pressure, where band “e'” almost entirely vanishes at the highest pressures. Remnants of the molecular peak persist up to ~20 GPa, partially overlapping to the polymeric “f” band.

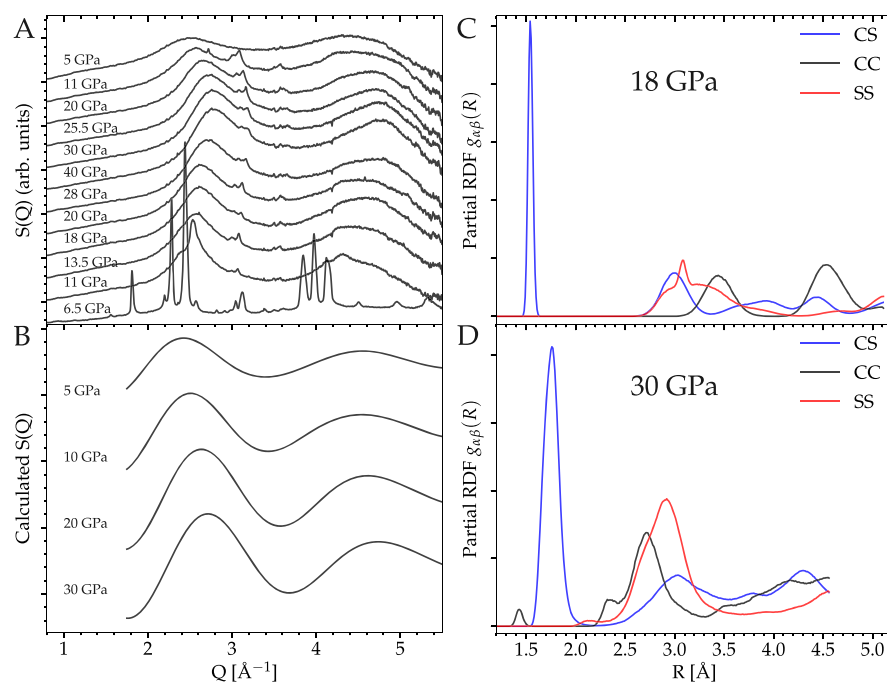


Figure 2. (A) Selected $S(Q)$ patterns of solid CS_2 measured, through XRD, along a typical pressure cycle: 6.5–40–5.0 GPa. (B) $S(Q)$ obtained from ab initio MD simulations. (C and D) computationally (MD) obtained partial radial distribution functions (RDFs), calculated for the $Cmce$ molecular crystal at 18 GPa (panel (C)) and for the polymeric sample at 30 GPa (panel (D)).

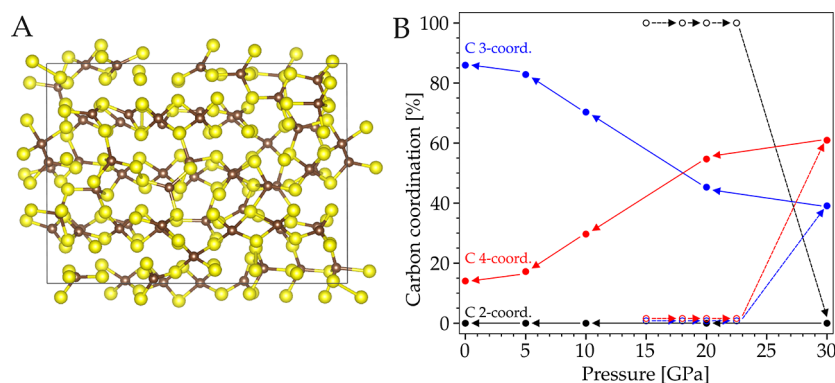


Figure 3. (Left) Structure of polymeric CS_2 from ab initio MD after polymerization of the $Cmce$ molecular crystal at 30 GPa. Right: fraction of C atoms with different coordination, as function of pressure from ab initio MD. Open and full circles are obtained upon increasing and decreasing pressure, respectively.

Then, the molecular peak is slightly enhanced when reducing pressure below 10 GPa, indicating the backformation of a very small amount of molecular CS_2 , a feature not readily observable through the much noisier Raman spectra. In fact, bands “e” and “f” already provide a few key insights on the chemical nature of polymeric CS_2 . Band “e” is compatible with the IR peak observed previously (see ref 21 and references therein) and empirically assigned to the $\text{C}=\text{S}$ stretching mode of the Bridgman’s polymer, $(-\text{C}(\text{S})-\text{S}-)_n$, while band “f” indicates the presence of $\text{C}=\text{C}$ double bonds. Therefore, bands “e” and “f” point to C in planar, 3-fold coordination, which appears suddenly above the polymerization pressure and then has a tendency to decrease upon increasing the pressure reversibly.

For directly proving the disordered character of polymeric CS_2 , we performed synchrotron XRD measurements. In Figure 2A, we report selected patterns of the static structure factor, $S(Q)$, of solid CS_2 measured along a typical pressure cycle in

the 5–40 GPa range, which significantly enrich the set of data reported in ref 22. At 6.5 GPa, we observe only the sharp Bragg peaks of the CS_2 molecular crystal ($Cmce$).³⁶ While in stark contrast, at 11 GPa, we observe a glassy-like $S(Q)$ dominated by two broad peaks at around 2.5 \AA^{-1} and 4.5 \AA^{-1} ; the peak at 2.5 \AA^{-1} is very close to the still visible strongest Bragg peaks of the molecular phase. The change is complete at 13.5 GPa where, besides the two broad diffuse peaks, we also observe, at all pressures, very weak Bragg peaks at $3.0\text{--}3.6 \text{ \AA}^{-1}$, signaling the presence of minor extended crystalline phases (to be discussed later). These changes show, consistently with Raman and IR investigations, that CS_2 undergoes a major transformation to a disordered material above 10 GPa. The half width at half-maximum of the diffuse peak at lowest Q s amounts to $0.25\text{--}0.30 \text{ \AA}^{-1}$, implying a spatial coherence length of $\sim 3.3\text{--}4.0 \text{ \AA}$ or longer.

In order to better understand the structural transformation of the molecular crystal and the subsequent evolution of the

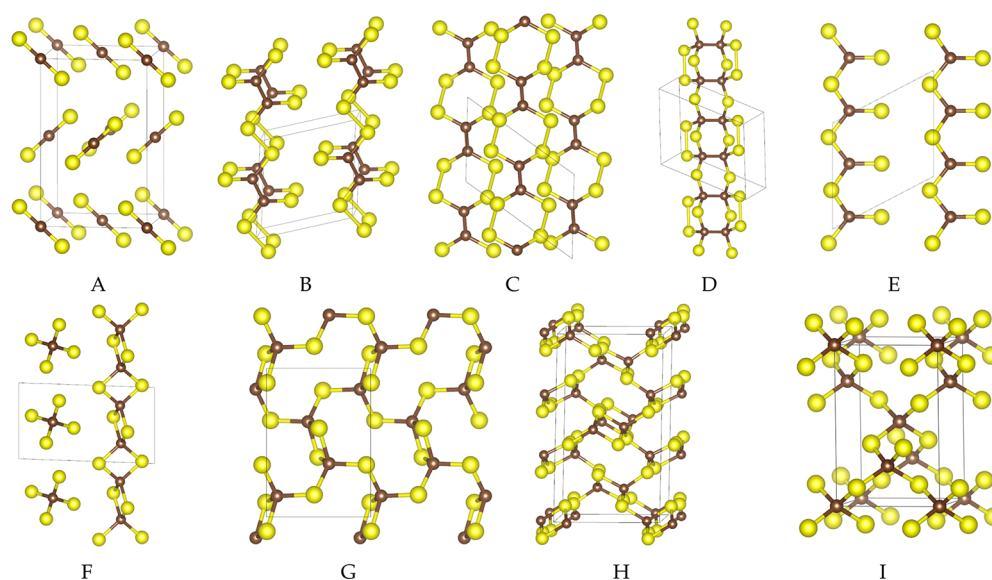


Figure 4. Selected structures found by evolutionary search: (A) *Cmce* molecular crystal,³⁶ (B) Frapper polymer,²⁴ (C) double Frapper polymer, (D) 262 chain, (E) Bridgman's black polymer,¹⁸ (F) SiS₂ NP like chain,³⁷ (G) shahabite,⁶ (H) *P2₁/c*, (I) β -cristobalite. A is molecular, B through F are linear polymers, G is layered, and H and I are extended systems. In structures B, C, and E, all carbon atoms are in 3-fold coordination, whereas in structures D, F, G, H, and I, they are all in 4-fold coordination.

disordered polymeric sample with pressure, we performed ab initio simulations. We started with direct compression of the *Cmce* sample³⁶ consisting of 192 atoms using ab initio MD. The protocol is shown in Figure S1 in the Supporting Information. Because of the well-known time-scale-gap problem, the sample did not transform at pressure close to the experimental value of 11 GPa and polymerization occurred upon overpressurization to 30 GPa. The resulting sample is a disordered polymeric system consisting of 3-fold and 4-fold coordinated carbon atoms (Figure 3A). It can be seen that there is still visible medium-range order in the positions of S atoms, originating from the molecular phase while C atoms seem to be more disordered. The polymerized structure was then decompressed to 20, 10, 5 and 0 GPa in order to check for potential pressure-induced structural changes. Figure 3B shows the evolution of the number of C atoms in molecular 2-fold (C2) and in polymeric planar 3-fold (C3) and tetrahedral 4-fold (C4) coordination upon compression and decompression. Immediately after polymerization at 30 GPa, the system contains ~61% C4 atoms and 39% C3 atoms. Upon decompression, this ratio reverts below 20 GPa and at 5 GPa almost 83% of C atoms are 3-fold coordinated. In Figure 2, we show a comparison of the $S(Q)$, calculated from our samples (Figure 2B), to the experimental one obtained from XRD (Figure 2A). The Q positions of the first two broad peaks of the calculated $S(Q)$ compare fairly well to those of the experimental structure factor and the evolution upon decompression also follows closely the experimental behavior. Incidentally, we note that, because of the limited experimental Q range, experimental XRD data did not allow us to obtain RDFs for reliable determination of the local structure and, particularly, for accurate identification of the relevant chemical bonds. In Figure 2, we also report the computationally obtained partial RDFs, calculated for the *Cmce* molecular crystal at 18 GPa (Figure 2C) and for the polymeric sample at 30 GPa (Figure 2D). Remarkably, the position of the nearest neighbors' C-S peak increases from 1.54 Å in the molecular crystal to 1.76 Å in polymeric CS₂, indicating breaking or

weakening of the molecular C=S double bonds. Also, the existence of C=C nearest neighbors' in the polymer, although very limited, is supported by a peak at 1.43 Å in the CC partial RDF.

In order to compare computational results to the experimental Raman and IR spectra, we further calculated the vibrational density of states (VDOS) for the disordered samples at 30, 20, 10 and 5 GPa. VDOS represents a proxy to Raman and IR spectra, particularly for amorphous materials. The results are shown in Figures 1C (30 GPa) and 1D (10 GPa). By analyzing the partial contributions to VDOS, one can identify specific signatures of atoms with different coordination and different chemical environment. Based on VDOS, we can assign the Raman and IR peaks as follows: peaks "a" and "b" around 130 cm⁻¹ and 500 cm⁻¹, respectively, mainly come from S atoms (S2) bridging two C atoms. The broad peak *c* at 600–800 cm⁻¹ mainly encodes contributions from 4-fold coordinated C atoms (C4). We note that, similar to the experiment, the intensity of this peak decreases upon decreasing the pressure, revealing the drop of carbon coordination from 4 to 3. The broad peaks "d" and "e" at 800–1100 cm⁻¹ encode contributions from 3-fold coordinated C atoms (C3). The intensity evolution of this peak with pressure is inverse to that of peak "c", which further supports the change of coordination of C from 3-fold, at low pressures, to 4-fold at higher pressures. Peak "f" is traced back to C3 sites and, particularly, to C=C double bonds and the reversible intensity drop of this peak upon increasing pressure signals once more reversible C3-to-C4 changes in local structure. The fine structure of the peak "b" at ~500 cm⁻¹ provides another fingerprint of the population balance between C3 and C4 carbon atoms. In the Raman spectra, right after the transition at 11.2 and 14.5 GPa, this peak has a shoulder at ~550 cm⁻¹. Upon increasing the pressure, the shoulder of peak "b" drops and eventually disappears. In Figure S2 in the Supporting Information, we show the contributions from sulfur bridging two C atoms, which can be either C3 or C4. The C3-S2-C3 and C4-S2-C3 configurations produce a peak at 550 cm⁻¹

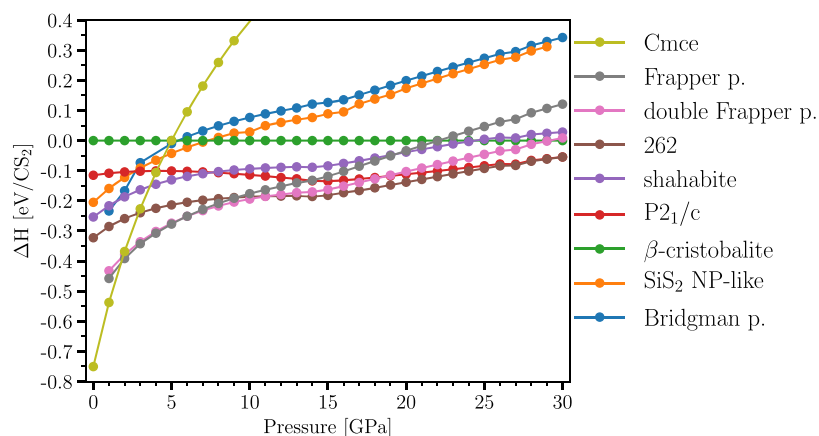


Figure 5. Enthalpy versus pressure for selected crystal structures of polymeric CS₂ found with evolutionary search. Enthalpy is relative to the β -cristobalite structure.

while the C4-S2-C4 configuration produces a peak at 500 cm⁻¹. The change of shape of the experimental Raman peak “b” upon compression thus also directly reflects the change in the proportion of C3 and C4 carbon atoms.

To rationalize the observed pressure evolution trends by thermodynamics, we performed an evolutionary search of crystal structures of stoichiometric CS₂ in the low-pressure range of 5–10 GPa, not covered in previous studies.^{25,26} Selected crystal structures found in the search are shown in Figure 4, and their enthalpies are reported in Figure 5, as a function of pressure. We first note that, already at 5 GPa, the enthalpies of the *Cmce* molecular crystal (Figure 4A), the C3 structure (made of BBP) (Figure 4E) and the tetrahedral C4 β -cristobalite structure (Figure 4I) cross each other. Surprisingly, the widely accepted BBP is not a good structure at any pressure, and beyond 5 GPa, it becomes the second worst structure right after the *Cmce* molecular crystal while all other structures containing C4 atoms have lower enthalpy. This explains the presence of C4 atoms right after polymerization at ~11 GPa and challenges the traditional view of nonmolecular CS₂ being a Bridgman polymer, where all C atoms are in 3-fold coordination. The lowest enthalpy structure in the low pressure range of 2–5 GPa is the polymer 11c predicted by Frapper, here named the Frapper polymer (snapshot shown in Figure 4B)²⁴ with a volume drop of 21% from the *Cmce* molecular crystal. A closely related structure arises by bonding remaining terminal sulfurs together, thus creating a chain with alternating C=C bonds and double S–S bridges, which, here, we call a double Frapper polymer (see Figure 4C). This polymer is thermodynamically preferred in the pressure range of 6–11 GPa, although the difference between the single and the double Frapper polymers is very small, i.e., <0.01 eV/molecule. The carbon–carbon bond length is 1.46 Å and 1.37 Å in the former and latter polymer, respectively. The high stability of these polymers featuring direct bonds between two atoms of the same element rather than C–S bonds clearly reflects the metastability of the CS₂ molecule, with respect to decomposition. At the same time, the double Frapper polymer allows us to explain the origin of peak *f* in Raman and IR spectra. The presence of C=C bond results in the VDOS peak at 1400 cm⁻¹ (see Figure 1), suggesting that peak “*f*” can be explained as resulting mainly from plain polymerization (albeit with a different orientation of molecules), with no need for major chemical disproportionation. It is also natural that peaks “*e*” and “*f*”, which correspond to C=S and C=C double

bonds, disappear upon increasing pressure. On the other hand, the fact that peak “*f*” reappears even more strongly upon decompression reflects the thermodynamic instability toward decomposition, which may indeed partially occur upon decreasing pressure. The VDOS calculated for the crystal structures are shown in Figure S3 in the Supporting Information and provide further support for the assignment of the Raman and IR peaks.

The presence of both C3 and C4 carbon atoms right after polymerization at ~11 GPa can be further rationalized by looking for potential polymerization pathways in the parent *Cmce* molecular crystal. Inspection of close intermolecular C...S contacts (presented in detail in the Supporting Information (see Figure S4)) points to the existence of several distinct and concurrently operating polymerization mechanisms. These provide a plausible explanation for the lack of order in the polymeric form, since the formation of a polymeric crystalline phase would instead require one mechanism being dominant, which appears unlikely.

We now turn back to the very weak Bragg peaks observed at 3.0–3.6 Å⁻¹, at >10 GPa (Figure 2A). In fact, none of the polymeric crystalline phases found through our evolutionary search and also none of the known crystalline phases of pure S and C fits these peaks. Therefore, it is more than natural to infer that this XRD pattern is likely not to belong to the stoichiometric CS₂ system nor to pure S or C, but it rather belongs either to a minor disproportionated C-rich C/S phase with carbon in planar coordination and likely C=C double bonds, or to a minor S-rich C/S phase, or even to some combination of both. These two types of crystalline phases would certainly contribute to the vibrational band “*f*”, and to bands “*a*” and “*b*”, respectively. Following this interpretation, the slight intensity increase of the mentioned Bragg peaks observed upon decreasing pressure reasonably indicates the progressive disproportionation of polymeric CS₂, which was also inferred above from the investigation of vibrational modes.

Our study shows that the structure of disordered polymeric CS₂ is more complex than previously thought. At the polymerization pressure threshold, 10–11 GPa, C4 atoms are already thermodynamically preferred to C3 atoms and BBP-like chains thus appear for kinetic reasons only. The polymeric network consists of a mixture of C3 and C4 atoms (with C4/C3 ratio increasing with pressure), which is one of the key factors contributing to the structural disorder in the system. At the same time, the network partially retains some

order of S atoms from the parent molecular crystal. The main structural transformations observed upon compression up to 40 GPa can be explained without assuming major chemical disproportionation. The structural disorder naturally arises from the presence of several competing polymerization pathways in the *Cmce* molecular crystal, suggesting that the synthesis of polymeric CS₂ in a crystalline phase likely remains a challenge.

■ ASSOCIATED CONTENT

SI Supporting Information

The Supporting Information is available free of charge at <https://pubs.acs.org/doi/10.1021/acs.jpcllett.1c01762>.

- (I) Methods; (II) Ab initio molecular dynamics compression and decompression; (III) Partial VDOS; (IV) Polymerization mechanism (PDF)

■ AUTHOR INFORMATION

Corresponding Author

Mario Santoro – Key Laboratory of Materials Physics, Institute of Solid State Physics, Chinese Academy of Sciences, Hefei 230031, China; Istituto Nazionale di Ottica (CNR-INO) and European Laboratory for non Linear Spectroscopy (LENS), 50019 Sesto Fiorentino, Italy; orcid.org/0000-0001-5693-4636; Email: santoro@lens.unifi.it

Authors

Jinwei Yan – Key Laboratory of Materials Physics, Institute of Solid State Physics, Chinese Academy of Sciences, Hefei 230031, China; University of Science and Technology of China, Hefei 230026, China; Center for High Pressure Science and Technology Advanced Research, Shanghai 201203, China

Ondrej Tóth – Department of Experimental Physics, Faculty of Mathematics, Physics and Informatics, Comenius University in Bratislava, 842 48 Bratislava, Slovakia

Wan Xu – Key Laboratory of Materials Physics, Institute of Solid State Physics, Chinese Academy of Sciences, Hefei 230031, China; University of Science and Technology of China, Hefei 230026, China

Xiao-Di Liu – Key Laboratory of Materials Physics, Institute of Solid State Physics, Chinese Academy of Sciences, Hefei 230031, China

Eugene Gregoryanz – Key Laboratory of Materials Physics, Institute of Solid State Physics, Chinese Academy of Sciences, Hefei 230031, China; School of Physics and Astronomy and Centre for Science at Extreme Conditions, University of Edinburgh, Edinburgh EH9 3JZ, U.K.; Center for High Pressure Science and Technology Advanced Research, Shanghai 201203, China

Philip Dalladay-Simpson – Center for High Pressure Science and Technology Advanced Research, Shanghai 201203, China

Zeming Qi – National Synchrotron Radiation Laboratory, University of Science and Technology of China, Hefei 230029, China

Shiyu Xie – National Synchrotron Radiation Laboratory, University of Science and Technology of China, Hefei 230029, China

Federico Gorelli – Key Laboratory of Materials Physics, Institute of Solid State Physics, Chinese Academy of Sciences, Hefei 230031, China; Center for High Pressure Science and

Technology Advanced Research, Shanghai 201203, China; Istituto Nazionale di Ottica (CNR-INO) and European Laboratory for non Linear Spectroscopy (LENS), 50019 Sesto Fiorentino, Italy

Roman Martoňák – Department of Experimental Physics, Faculty of Mathematics, Physics and Informatics, Comenius University in Bratislava, 842 48 Bratislava, Slovakia; orcid.org/0000-0002-4013-9117

Complete contact information is available at: <https://pubs.acs.org/doi/10.1021/acs.jpcllett.1c01762>

Notes

The authors declare no competing financial interest.

■ ACKNOWLEDGMENTS

O.T. and R.M. were supported by the VEGA project (No. 1/0640/20) and the Slovak Research and Development Agency, under Contract No. APVV-19-0371. Calculations were performed at the Computing Centre of the Slovak Academy of Sciences using the supercomputing infrastructure acquired in ITMS Projects No. 26230120002 and No. 26210120002 (Slovak Infrastructure for High-Performance Computing) supported by the Research and Development Operational Programme funded by the ERDF. This work was supported by Youth Innovation Promotion Association of CAS (No. 2021446), National Natural Science Foundation of China (Grant Nos. 11874361, 51672279, 51727806 and 11774354), Innovation Grant of CAS (No. CXJJ-19-B08), Science Challenge Project (No. TZ2016001), CASHIPS Director's Fund (Grant No. YZJJ201705) and CAS President's International Fellowship Initiative Fund (No. 2019VMA0027).

■ REFERENCES

- (1) Hemley, R. J.; Prewitt, C. T.; Kingma, K. J. In *Silica*; Heaney, P. J., Prewitt, C. T., Gibbs, G. V., Eds.; De Gruyter, 2018; pp 41–82.
- (2) Prokopenko, V.; Dubrovinsky, L.; Dmitriev, V.; Weber, H.-P. In situ characterization of phase transitions in cristobalite under high pressure by Raman spectroscopy and X-ray diffraction. *J. Alloys Compd.* **2001**, *327*, 87–95.
- (3) Haines, J.; Léger, J. M.; Gorelli, F.; Hanfland, M. Crystalline Post-Quartz Phase in Silica at High Pressure. *Phys. Rev. Lett.* **2001**, *87*, 155503.
- (4) Durben, D. J.; Wolf, G. H. Raman spectroscopic study of the pressure-induced coordination change in GeO₂ glass. *Phys. Rev. B: Condens. Matter Mater. Phys.* **1991**, *43*, 2355–2363.
- (5) Guthrie, M.; Tulk, C. A.; Benmore, C. J.; Xu, J.; Yarger, J. L.; Klug, D. D.; Tse, J. S.; Mao, H.-k.; Hemley, R. J. Formation and Structure of a Dense Octahedral Glass. *Phys. Rev. Lett.* **2004**, *93*, 115502.
- (6) Plašienka, D.; Martoňák, R.; Tosatti, E. Creating new layered structures at high pressures: SiS₂. *Sci. Rep.* **2016**, *6*, 37694.
- (7) Evers, J.; Möckl, L.; Oehlinger, G.; Köppe, R.; Schnöckel, H.; Barkalov, O.; Medvedev, S.; Naumov, P. More Than 50 Years after Its Discovery in SiO₂ Octahedral Coordination Has Also Been Established in SiS₂ at High Pressure. *Inorg. Chem.* **2017**, *56*, 372–377.
- (8) Wang, Y.; Jiang, S.-Q.; Goncharov, A. F.; Gorelli, F. A.; Chen, X.-J.; Plašienka, D.; Martoňák, R.; Tosatti, E.; Santoro, M. Synthesis and Raman spectroscopy of a layered SiS₂ phase at high pressures. *J. Chem. Phys.* **2018**, *148*, 014503.
- (9) Iota, V.; Yoo, C. S.; Cynn, H. Quartzlike Carbon Dioxide: An Optically Nonlinear Extended Solid at High Pressures and Temperatures. *Science* **1999**, *283*, 1510–1513.
- (10) Santoro, M.; Gorelli, F. A.; Bini, R.; Ruocco, G.; Scandolo, S.; Crichton, W. A. Amorphous silica-like carbon dioxide. *Nature* **2006**, *441*, 857.

- (11) Montoya, J. A.; Rousseau, R.; Santoro, M.; Gorelli, F.; Scandolo, S. Mixed Threefold and Fourfold Carbon Coordination in Compressed CO₂. *Phys. Rev. Lett.* **2008**, *100*, 163002.
- (12) Santoro, M.; Gorelli, F. A.; Bini, R.; Haines, J.; Cambon, O.; Levelut, C.; Montoya, J. A.; Scandolo, S. Partially collapsed cristobalite structure in the non molecular phase V in CO₂. *Proc. Natl. Acad. Sci. U. S. A.* **2012**, *109*, 5176–5179.
- (13) Datchi, F.; Mallick, B.; Salamat, A.; Ninet, S. Structure of Polymeric Carbon Dioxide CO₂-V. *Phys. Rev. Lett.* **2012**, *108*, 125701.
- (14) Plašienka, D.; Martoňák, R. Structural evolution in high-pressure amorphous CO₂ from ab initio molecular dynamics. *Phys. Rev. B: Condens. Matter Mater. Phys.* **2014**, *89*, 134105.
- (15) Shieh, S. R.; Jarrige, I.; Wu, M.; Hiraoka, N.; Tse, J. S.; Mi, Z.; Kaci, L.; Jiang, J.-Z.; Cai, Y. Q. Electronic structure of carbon dioxide under pressure and insights into the molecular-to-nonmolecular transition. *Proc. Natl. Acad. Sci. U. S. A.* **2013**, *110*, 18402–18406.
- (16) Lee, M.-S.; Montoya, J. A.; Scandolo, S. Thermodynamic stability of layered structures in compressed CO₂. *Phys. Rev. B: Condens. Matter Mater. Phys.* **2009**, *79*, 144102.
- (17) Bridgman, P. W. Freezing Parameters and Compressions of Twenty-One Substances to 50,000 Kg/Cm². *Proceedings of the American Academy of Arts and Sciences* **1942**, *74*, 399–424.
- (18) Whalley, E. Structure of Bridgman's Black Carbon Disulphide. *Can. J. Chem.* **1960**, *38*, 2105–2108.
- (19) BUTCHER, E. G.; ALSOP, M.; WESTON, J. A.; GEBBIE, H. A. Formation and Properties of the Black Form of Carbon Disulphide. *Nature* **1963**, *199*, 756–758.
- (20) Chan, W. S.; Jonscher, A. K. Structural and Electrical Properties of Solid Polymeric Carbon Disulphide. *Phys. Status Solidi B* **1969**, *32*, 749–761.
- (21) Agnew, S. F.; Mischke, R. E.; Swanson, B. I. Pressure- and temperature-induced chemistry of carbon disulfide. *J. Phys. Chem.* **1988**, *92*, 4201–4204.
- (22) Dias, R. P.; Yoo, C.-S.; Kim, M.; Tse, J. S. Insulator-metal transition of highly compressed carbon disulfide. *Phys. Rev. B: Condens. Matter Mater. Phys.* **2011**, *84*, 144104.
- (23) Dias, R. P.; Yoo, C.-S.; Struzhkin, V. V.; Kim, M.; Muramatsu, T.; Matsuoka, T.; Ohishi, Y.; Sinogeikin, S. Superconductivity in highly disordered dense carbon disulfide. *Proc. Natl. Acad. Sci. U. S. A.* **2013**, *110*, 11720–11724.
- (24) Frapper, G.; Saillard, J.-Y. Search for New Allotropic Forms of Carbon Dioxide and Carbon Disulfide: A Density Functional Study of CX₂-Based Oligomers (X = O, S). *J. Am. Chem. Soc.* **2000**, *122*, 5367–5370.
- (25) Naghavi, S. S.; Crespo, Y.; Martoňák, R.; Tosatti, E. High-pressure layered structure of carbon disulfide. *Phys. Rev. B: Condens. Matter Mater. Phys.* **2015**, *91*, 224108.
- (26) Zarifi, N.; Liu, H.; Tse, J. S. Structures of the metallic and superconducting high pressure phases of solid CS₂. *Sci. Rep.* **2015**, *5*, 10458.
- (27) Zarifi, N.; Tse, J. S. Structural Search for High Pressure CS₂ and Xe–Cl Compounds. *J. Phys. Soc. Jpn.* **2018**, *87*, 041014.
- (28) Mao, H. K.; Bell, P. M.; Shaner, J. W.; Steinberg, D. J. Specific volume measurements of Cu, Mo, Pd, and Ag and calibration of the ruby R1 fluorescence pressure gauge from 0.06 to 1 Mbar. *J. Appl. Phys.* **1978**, *49*, 3276–3283.
- (29) Akahama, Y.; Kawamura, H. Pressure calibration of diamond anvil Raman gauge to 310 GPa. *J. Appl. Phys.* **2006**, *100*, 043516.
- (30) Oganov, A. R.; Glass, C. W. Crystal structure prediction using ab initio evolutionary techniques: Principles and applications. *J. Chem. Phys.* **2006**, *124*, 244704.
- (31) Oganov, A. R.; Lyakhov, A. O.; Valle, M. How Evolutionary Crystal Structure Prediction Works—and Why. *Acc. Chem. Res.* **2011**, *44*, 227–237.
- (32) Kresse, G.; Hafner, J. Ab initio molecular dynamics for liquid metals. *Phys. Rev. B: Condens. Matter Mater. Phys.* **1993**, *47*, 558–561.
- (33) Kresse, G.; Furthmüller, J. Efficiency of ab-initio total energy calculations for metals and semiconductors using a plane-wave basis set. *Comput. Mater. Sci.* **1996**, *6*, 15–50.
- (34) Perdew, J. P.; Burke, K.; Ernzerhof, M. Generalized Gradient Approximation Made Simple. *Phys. Rev. Lett.* **1996**, *77*, 3865–3868.
- (35) Tkatchenko, A.; Scheffler, M. Accurate Molecular Van Der Waals Interactions from Ground-State Electron Density and Free-Atom Reference Data. *Phys. Rev. Lett.* **2009**, *102*, 073005.
- (36) Baenziger, N. C.; Duax, W. L. Crystal Structure and Molecular Motion of Solid Carbon Disulfide. *J. Chem. Phys.* **1968**, *48*, 2974–2981.
- (37) Büssem, W.; Fischer, H.; Gruner, E. Die Struktur des Siliciumdisulfids. *Naturwissenschaften* **1935**, *23*, 740–740.